Harmful Algae 148 (2025) 102922

Contents lists available at ScienceDirect

Harmful Algae

journal homepage: www.elsevier.com/locate/hal

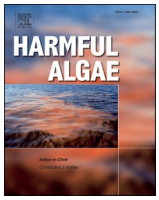

Transcriptional responses to oxygen gradients in cyanobacterial aggregates

Dezhuang Gao [a,b,c], Zhijie Chen [a,b,c,#], Yuan Ma [a], Ruiyu Wang [a], Jie Deng [a,b,c,*]

[a] Zhejiang Tiantong Forest Ecosystem National Observation and Research Station, Center for Global Change and Ecological Forecasting, School of Ecological and Environmental Sciences, East China Normal University, Shanghai, China
[b] Technology Innovation Center for Land Spatial Eco-restoration in Metropolitan Area, Ministry of Natural Resources, Shanghai, China
[c] Institute of Eco-Chongming, Shanghai, China

ARTICLE INFO

Keywords:
Cyanobacterial aggregates
Phycospheric microorganisms
Cyanobacterial bloom
Dissolved oxygen level
Microcystis

ABSTRACT

Cyanobacterial aggregates (CAs) are the main cause of harmful cyanobacterial blooms in freshwater lakes, posing serious risks to water quality and ecosystem health. The ecological success of CAs is closely linked to their abilities to adapt to fluctuating dissolved oxygen (DO) levels. In this study, we investigated the transcriptional responses of CA-associated microbial communities across a gradient of DO concentrations (0–6 mg/L) using incubation experiments combined with 16S rRNA transcript and metatranscriptomic sequencing. Distinct transcriptional patterns of clusters of genes were revealed for both cyanobacterial and phycospheric communities. Notably, *Microcystis*, the dominating cyanobacteria in the CAs, demonstrated markedly elevated transcriptional activities under oxygen-deficient conditions. Under low DO, cyanobacteria actively cope with reactive oxygen species (ROS) stress, and utilized fermentation and O_2-independent alternative electron sink to maintain anaerobic metabolism. Upregulation of gas vesicle protein genes also suggests a role in buoyancy regulation to escape low-oxygen zones. These transcriptomic findings were further supported by physiological assays of *Microcystis*, which exhibited increased ROS level, extracellular polysaccharides (EPS) content and alcohol production under oxygen-deficient conditions. Moreover, intensified competition for nutrients between cyanobacteria and phycospheic bacteria under low DO were revealed, although the latter may also support cyanobacterial growth through cobalamin (vitamin B_{12}) provisioning. Collectively, our findings uncover key adaptive responses of *Microcystis* under oxygen-deficient conditions and underscore the importance of redox regulation in shaping the metabolic dynamics of CA-associated microbial communities.

1. Introduction

Harmful algal blooms (HABs) are dense accumulations of algae that occur in aquatic environments largely affected by eutrophication and climate change factors (Gobler, 2020). The increasing frequency and intensity of HABs worldwide poses significant threats to ecosystem balance and human health, causing economic impacts and water treatment challenges (Feng et al., 2024). In freshwater ecosystems, *Microcystis* is one of the most common bloom-forming cyanobacteria, typically forming colonies with diverse phycospheric microorganisms embedded in a mucilage matrix, collectively referred to as cyanobacterial aggregates (CAs) (Xiao et al., 2018). The formation of CAs involves both cell division and adhesion processes, which may be influenced by biotic factors such as zooplankton grazing and the presence of heterotrophic bacteria, as well as abiotic factors including temperature, light intensity, and metal ion concentrations (Xiao et al., 2018). CAs offer significant advantages over single cells by better adaptation to varying light conditions, increased resistance to water flow and predation, sustained growth under nutrient limitation, and enhanced buoyancy (Hajdu et al., 2007; Ma et al., 2014; Paerl et al., 2011; Walsby et al., 1997). However, the mechanisms by which CAs adapt to variations in oxygen levels were often overlooked.

The microchemical environment within CAs, particularly the redox environment, is highly complex largely owing to the aggregate structure. During daylight, intense photosynthesis by cyanobacteria, combined with limited oxygen diffusion, leads to accumulation of oxygen within CAs. The excessive oxygen molecules passively diffuse into cells, enhancing the rate of electron transfer in the aerobic respiratory chain.

* Corresponding author at: School of Ecological and Environmental Sciences, East China Normal University, Shanghai, China.
E-mail address: jdeng@des.ecnu.edu.cn (J. Deng).
# Equal contribution as first author.

https://doi.org/10.1016/j.hal.2025.102922
Received 5 December 2024; Received in revised form 28 June 2025; Accepted 3 July 2025
Available online 5 July 2025

In the meanwhile, reactive oxygen species (ROS), such as superoxide anions (O_2^-) and hydrogen peroxide (H_2O_2), are produced due to over-reduction of the photosynthetic electron transport chain, potentially leading to cellular damage (Latifi et al., 2009; Yang et al., 2023). Conversely, under low light or dark conditions, the rate of oxygen diffusion into CAs cannot compensate the rate of oxygen consumption by microbial respiration inside the CAs. This imbalance can create hypoxic or even anoxic centers within CAs, producing an oxygen gradient from the CA centers to the surfaces (Bianchi et al., 2018; Klawonn et al., 2015; Wu et al., 2023).

The motility of CAs also subjects them to fluctuating oxygen levels. For instance, CAs dominated by gas-vesiculating cyanobacteria exhibit significant vertical migration capabilities, allowing them to move within the water column (Pfeifer, 2012). This motility helps cyanobacteria access more oxygen, sunlight, and carbon dioxide as they move towards the water surface. On the contrary, if the buoyancy provided by gas vesicles is insufficient to counteract the increased cell density due to accumulation of carbohydrates, the cells would sink toward deeper water with lower oxygen availability (Latour et al., 2004; Walsby and Booker, 1980; Wu et al., 2023). Consequently, the microbes residing in CAs frequently experience shifts among oxic, hypoxic, and even anoxic conditions. These conditions may lead to significant changes in active community structure, interspecific interactions, and metabolic activities of CAs. Hence, the ability of CA-associated microorganisms to adapt to fluctuating oxygen levels is crucial for sustaining the ecological dominance of CAs throughout the bloom period.

Under conditions when CAs are exposed to high oxygen concentrations, the generation of ROS can lead to cellular damage and disrupt biochemical processes. Cyanobacteria can employ both non-enzymatic and enzymatic antioxidants to counteract excessive ROS. Non-enzymatic antioxidants include compounds such as carotenoids and ascorbate (vitamin C), while enzymatic antioxidants involve superoxide dismutases (SOD), catalases, et cetera (Rai et al., 2025). Within CAs, the ability of cyanobacteria to maintain normal metabolic functions under ROS stress may also be partly attributed to synergistic cooperation with phycospheric bacteria (Latour et al., 2004; Morris et al., 2011). For instance, Biller et al. found that co-culturing the marine bacterium *Alteromonas macleodii* with the cyanobacterium *Prochlorococcus* reduced the stress level in *Prochlorococcus* (Biller et al., 2016). Similarly, Christie-Oleza et al. observed that when *Synechococcus* was co-cultured with heterotrophic bacteria, the expression of genes encoding stress-related proteins such as catalase-peroxidase, peroxiredoxin and superoxide dismutase decreased, supporting that *Synechococcus* can adjust its stress response strategies based on the presence or absence of heterotrophic partners (Christie-Oleza et al., 2017).

Cyanobacteria also have adaptive strategies under hypoxic or anoxic environments. For example, *Microcystis* can transform to dormant state to survive overwinter in lake sediment, which is characterized of oxygen deficiency and darkness (Robarts and Zohary, 1987). *Synechococcus* can survive in the anoxic dark waters of the Black Sea owing to its capability of fermentation (Callieri et al., 2019; Chuang and Liao, 2021). It was even reported that nitrate assimilation may provide an alternative electron sink for *Synechocystis* under anoxia(Gutthann et al., 2007). However, despite the above findings, understanding of adaptation strategies of cyanobacteria under oxygen-deficient conditions remain rare (Guerrero and Berlanga, 2016; Hoffmann et al., 2015).

So far, limited studies have investigated the changes of cyanobacterial metabolism or bacteria-cyanobacteria relationship under varying oxygen levels. To simulate the dissolved oxygen variations that CAs may experience in the water column—resulting in complex dissolved oxygen (DO) gradients within the aggregates—an incubation system capable of maintaining stable DO levels was established. CAs were incubated under a range of DO levels, and the metabolic responses of CA-associated microorganisms were investigated using both 16S rRNA transcript sequencing and metatranscriptomic sequencing approaches. The findings of this study shall provide insights into the metabolic mechanisms of CAs in response to fluctuating oxygen levels, which are crucial for their fitness and ability to maintain ecological dominance during cyanobacterial blooms.

2. Methods

2.1. Experimental design

CA samples were collected on September 22, 2022, from Dianshan Lake, Shanghai during a *Microcystis* bloom (31°4′49″ N, 121°54′27″ E). Presence of *Microcystis* aggregates was confirmed by both visual inspection and microscopic examination [**Fig. S1**]. Lake water was filtered through a 40 mesh sieve to obtain CA particles above 400 μm in diameter. CAs were added to sterilized lake water with final concentrations of approximately 10^4 *Microcystis* cells/mL. *Microcystis* cell density was determined by counting individual cells after dispersing *Microcystis* aggregates into single cells using ultrasonic treatment. The samples were kept in darkness for 12 h prior to incubation, in order for the oxygen produced during photosynthesis within the aggregates to be consumed by microbial respiration. For the microcosm experiment, six gradients of DO levels were established, including 0, 1.2, 2.4, 3.6, 4.8 and 6 mg/L. For the anoxia (DO=0) treatment, samples were added into serum bottles and flushed with nitrogen gas for 10 min to remove oxygen, which were then sealed with butyl rubber stoppers and aluminum caps. For incubation under hypoxic and oxic conditions, the CA samples were transferred to conical flasks, and gently stirred with a magnetic stirrer [Fig. 1]. A DO probe was pre-cleaned with ethanol and inserted into the flask for continuous monitoring of DO during incubation. A micro-peristaltic pump was used to pump pre-filtered air into the conical flask at a constant rate. By adjusting the rate of air pumping to balance oxygen consumption by the CAs, different DO levels were maintained in the flasks. All incubations were conducted in the dark for six hours to allow sufficient time for transcriptional responses without inducing longer-term cellular adaptations such as dormancy. All treatments were performed in triplicates. At the end of incubation, the CAs were filtered through sterile 0.2 μm PES membrane filters, which were immediately frozen in liquid nitrogen. RNA extraction was performed within 48 h for all samples.

2.2. RNA extraction, metatranscriptomic and 16S rRNA amplicon sequencing

RNA was extracted using the Quick-RNATM Fecal/Soil Microprep kit (Zymo Research, USA) and treated with DNase I (lyophilized) (Zymo Research, USA) to remove DNA. The obtained RNA was examined using the NanoDrop One/OneC UV–Vis spectrophotometer (Thermo Fisher Scientific, USA), and the integrity was assessed using the Qubit 4 Fluorometer (Thermo Fisher Scientific, USA) with the Qubit RNA Integrity and Quality (IQ) Assay Kit (Thermo Fisher Scientific, USA) (Deben et al., 2013). Then, part of the RNA was reverse transcribed to cDNA using the HiScript III RT SuperMix (Vazyme, China).

For the cDNA samples, the 16S V4 region was amplified using the primer pair 515F and 806R with barcode ligated using the TaKaRa Premix Taq® Version 2.0 (TaKaRa Biotechnology Co., Dalian, China) (Caporaso et al., 2012). The amplicon sequencing library was constructed with the NEBNext® UltraTM II DNA Library Prep Kit for Illumina® (New England Biolabs, USA) according to the standard protocol. Sequencing was conducted with the Illumina Novaseq 6000 platform at Guangdong Magigene Biotechnology Co., Ltd. (Guangzhou, China). For metatranscriptomic sequencing, RNA replicate samples from each treatment were combined. Sequencing libraries were generated with the RNA samples using the ALFA-SEQ DNA Library Prep Kit (Findrop, China) according to the manufacturer's instructions. The library quality was evaluated using the Qubit 4.0 Fluorometer and the QSEP400 high-throughput nucleic acid and protein analysis system (Houze Biology Technology Co., China). Metatranscriptomic sequencing was

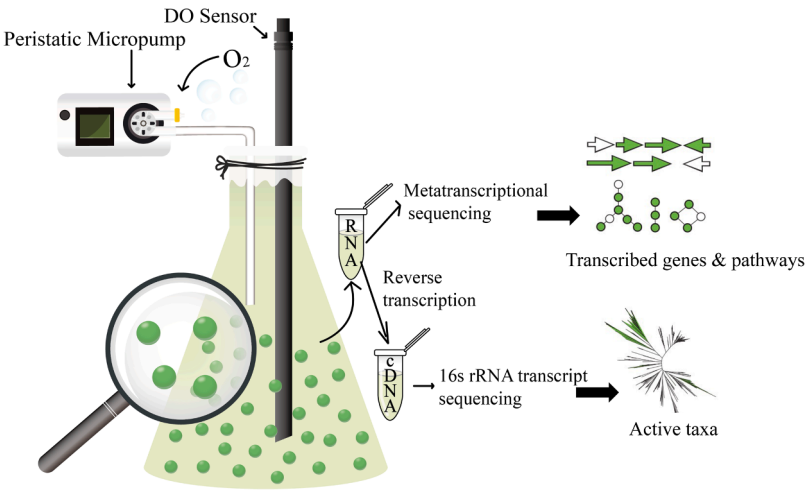

Fig. 1. A diagram of the cultivation system and the procedures for RNA extraction and sequencing. For the cultivation system, a DO probe was inserted into the flask for continuous monitoring of DO. Pre-filtered air was pumped into the flask with a micro-peristaltic pump at a constant rate. After RNA extraction, metatranscriptomic sequencing was used to investigate expression levels of genes and pathways. After reverse transcription to cDNA, amplicon sequencing of the 16S rRNA was performed to assess the composition of active CA-associated communities.

conducted at Novogene Co., Ltd. (Beijing). Data associated with this study were deposited at NODE database (the National Omics Data Encyclopedia: https://www.biosino.org/node) under project OEP005403.

2.3. Bioinformatic analyses

For the amplicon sequencing data, sequence profiles were processed using the QIIME 2 pipeline (QIIME 2 version: 2021.11) (Bolyen et al., 2019). In brief, raw sequences were demultiplexed and quality-controlled using the q2-demux plugin. The forward reads were truncated to 150 bases (–p-trunc-len-f 150) and the reverse reads were truncated to 147 bases (–p-trunc-len-r 147). DADA2 was employed for denoising, de-redundancy, and clustering of amplicon sequence variants (ASVs) (Callahan et al., 2016). ASVs matching mitochondria and chloroplasts were removed, and low-abundance sequences were filtered before rarefaction. Taxonomic assignment was performed using the feature-classifier classify-sklearn command against the Greengenes 13_8 99 % OTU reference sequences (Bokulich et al., 2018; McDonald et al., 2012).

For the metatranscriptomic data, the adapters of the raw sequences were removed using Trimmomatic (v0.39). The rRNA reads were removed by SortMeRNA (v4.2.0) (Bolger et al., 2014; Kopylova et al., 2012). The sequences were assembled using Trinity (v2.1.1), followed by gene prediction using Prodigal (v2.6.3) (Hyatt et al., 2010). Next, redundant sequences were removed using CD-HIT-EST (v4.8.1), and the remaining sequences were clustered at 95 % identity to obtain unique genes (Fu et al., 2012). The clean reads was mapped to the unique genes using Bowtie2 (v2.4.2) (Langmead and Salzberg, 2012). The SAM files were converted to BAM files and sorted using SAMtools (v1.7). Subsequently, BEDtools (v2.30.0) was used to obtain transcriptional abundances of unique genes in each sample, and gene abundances were calculated and converted to RPKM (Reads Per Kilobase of transcript per Million mapped reads) using Coverm (v0.6.1) with the following parameters:-min-read-aligned-percent 75 –min-read-percent-identity 95 –min-covered-fraction 10 –contig-end-exclusion 0 -m rpkm(Ji et al., 2024; Quinlan and Hall, 2010). Diamond (v2.0.5.143) were used for taxonomic classification(Buchfink et al., 2021). The genes were searched against the KO database using Diamond (v2.0.5.143) and mapped to the Kyoto Encyclopedia of Genes and Genomes (KEGG) for functional analysis (Kanehisa et al., 2004).

2.4. Metabolic assays

The metabolic responses of *Microcystis* were assessed under anoxic, hypoxic, and oxic conditions. The *Microcystis* strain FACHB-915 used in this study was obtained from the Freshwater Algae Culture Collection at the Institute of Hydrobiology of Chinese Academy of Sciences, Wuhan. DO levels in the flasks were maintained at approximately 1.5 mg/L and 7.4 mg/L for the hypoxic and oxic treatments, respectively. For the anoxic treatment, incubation was conducted in serum bottles, and flushed with N_2 gas before sealing. Three replicates were made for each treatment, and the incubation lasted 24 h. *Microcystis* cell counts were determined using a hemocytometer under a microscope. EPS levels were determined according to He et al. (He et al., 2020). Briefly, the culture was centrifuged at 4500 × *g* under 4 °C for 5 min, and the supernatant was discarded. PBS buffer (0.01 M) was added to restore the original volume, followed by heating at 55 °C in a water bath for 30 min. EPS content were measured using the anthrone-sulfuric acid method. Alcohol production and ROS levels were determined using the Ethanol Assay Kit (Beyotime, Catalog# S0240S, China) and the Reactive Oxygen Species Assay Kit (Beyotime, Catalog# S0033S, China), respectively.

2.5. Statistical analyses

Statistical analyses were primarily conducted in R versions 4.1.3 and 3.6.3. Principal Component Analysis (PCA) was performed using the 'FactoMineR' package (Le et al., 2008). Clustering analysis and visualization of the gene expression profiles were carried out using the 'ClusterGVis' package (Zhang, 2022). The clustering algorithm applied was 'mfuzz', and the optimal number of clusters was determined using the elbow method by calculating the Within-Cluster Sum of Squares (WSS).

3. Results

3.1. Variation of active microbial communities within CAs under different DO levels

Oxygen concentration was subjected to real-time monitoring throughout the duration of the experiment to ensure that the CAs were exposed to stable DO levels [**Fig. S2**]. Based on the 16S rRNA transcript profiles, reads associated with *Microcystis* accounted for 68–89 % in relative abundance in the whole community, suggesting absolute dominance of *Microcystis* [Fig. 2**A**]. A small fraction of

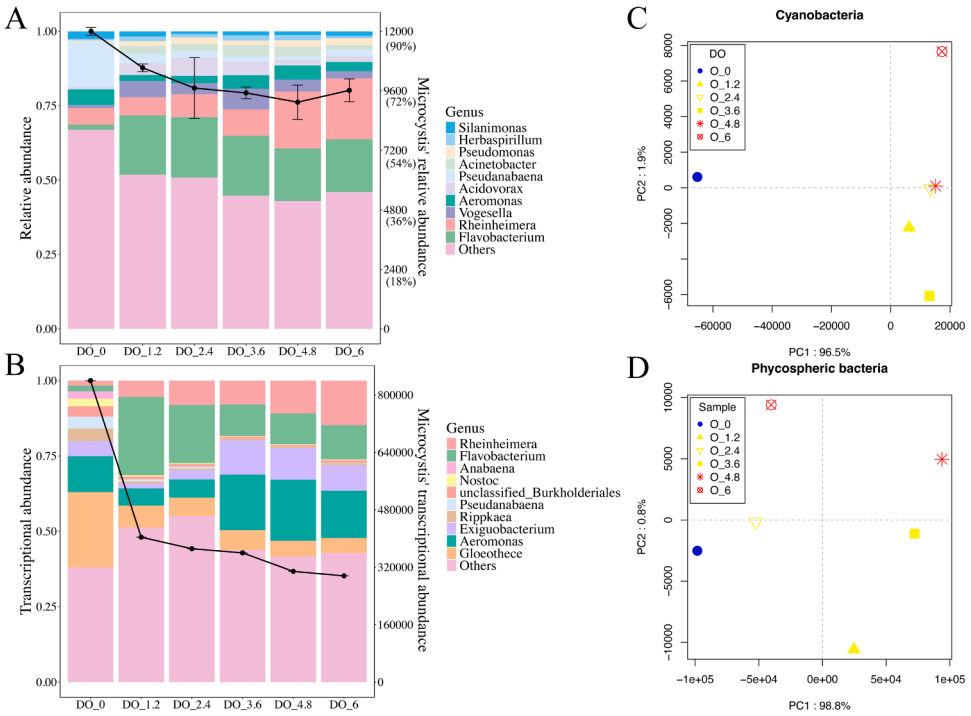

Fig. 2. Active microbial community structure within CAs under different DO levels. The black lines represent the abundance of *Microcystis* transcripts, while the stacked bars show those of the most abundant non-*Microcystis* genera based on the 16S rRNA (A) and metatranscriptomic profiles (B). "Others" refers to the sum of all other non-*Microcystis* taxa. The panels on the right are PCA results based on transcriptional profiles of cyanobacterial (C) and phycospheric bacterial (D) genes according to the metatranscriptomic analysis.

Pseudanabaenaceae was also found, ranging from 0.3 % to 1.5 % in relative abundance. The rest of the CA-associated communities were dominated by bacteria, while archaea only accounted for 0.01 %−0.02 % in relative abundance [**Table S1**]. Notably, the compositions of active communities in CAs under hypoxic (DO=1.2, 2.4 mg/L) and oxic (DO=3.6, 4.8, 6 mg/L) conditions were relatively similar, while showing marked difference with that under the anoxic condition (DO=0 mg/L) [Fig. 2**A**]. Both *Microcystis* and *Pseudanabaena* showed particularly high activities under anoxia. On the contrary, most phycospheric bacteria exhibited higher activities when oxygen was present, e.g., *Flavobacterium* and *Rheinheimera* [Fig. 2**A**]. Based on correlation analysis [Fig. 3], the abundance of *Microcystis* was positively correlated with *Pseudanabaena* ($p < 0.05$); while the abundances of phycospheric taxa including *Rheinheimera* and *Pseudomonas*, were positively correlated with DO concentration ($p < 0.05$). Additionally, correlations among phycospheric bacterial abundances were also observed. For example, the abundance of *Azohydromonas* was negatively correlated with those of many other phycosphere bacteria, while the abundance of

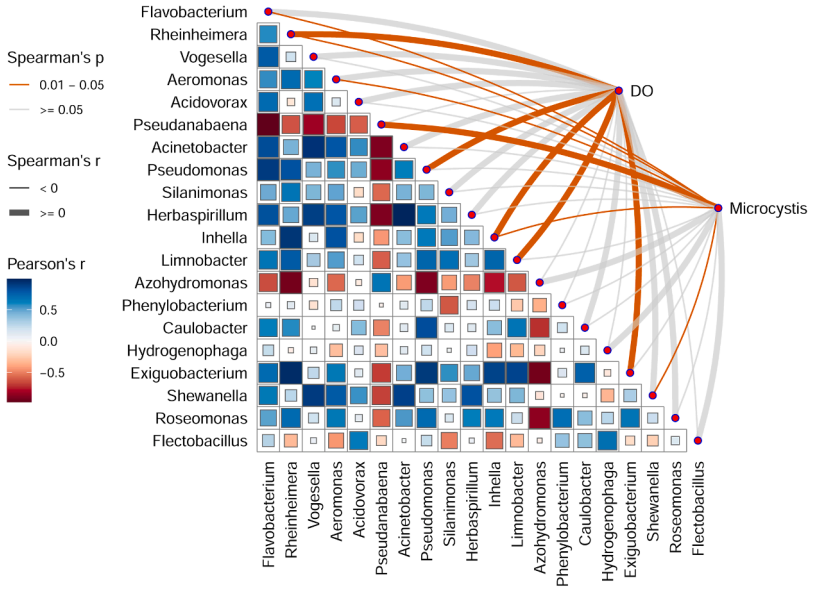

Fig. 3. Correlation analysis of CA-associated microbial abundances. The heatmap shows Pearson correlations among the abundances of the phycospheric taxa. Lines represent the correlations between the abundances of phycospheric taxa with *Microcystis* abundance and DO levels. The color and thickness of the lines indicate the *p*-value and correlation coefficient (r-value).

Roseomonas was positively correlated with the majority of phycospheric genera.

3.2. Gene expression patterns of CA-associated communities under anoxia

Metatranscriptomic sequencing was employed to investigate the metabolic response of CA-associated communities to different DO conditions. Consistent with the findings based on 16S rRNA transcript sequencing, the metatranscriptional profiles of cyanobacteria under anoxia was markedly different compared to hypoxic and oxic conditions [Fig. 2**AB**]. In comparison, the transcriptional profiles of phycospheric communities under anoxia did not differ as much relative to other DOs [Fig. 2**CD**]. Hence, characteristic response of cyanobacteria to anoxia was first assessed. Specifically, the transcriptional abundances of both *Pseudanabaena* and *Microcystis*, showed marked increase, suggesting these cyanobacteria were actively coping with anoxia [Fig. 2**B, S3**]. Notably, the expression of many genes associated with carbon metabolism, nutrient transport and assimilation in cyanobacteria had increased. This included fermentation pathways (pyruvate dikinase *ppsA*, alcohol dehydrogenase *adhCE* and lactate dehydrogenase *LDH*), the reductive pentose phosphate cycle, pyruvate oxidation, et cetera [Fig. 4, **S4, Table S2**]. The expression of a number of genes related to transporters and assimilatory processes were upregulated, too, including those for transporting nitrate/nitrite/cyanate (*nrtABCD*), phosphate (*pstABCS*), sulfate/thiosulfate (*sbp, cysAUW*) and iron (*afuABC*), as well as assimilatory nitrate (*narB, nirA*) and sulfate reduction (*sat, cysCH, sir*). In addition, transcription of many genes associated with redox balance was also more active under anoxia, such as those in the pentose phosphate pathway, the ones encoding the bidirectional [NiFe] hydrogenases (*hoxEFU*), NAD(P)H-quinone oxidoreductases (*ndhABCD*, among others), ferredoxin-associated proteins (*petFH*, among others) and the photosynthetic electron transport system (*psbABCDE, petABCDEFH, atpABEFH*, among others). Notably, the expression of the *sasA* and *rpaAB* genes responsible for sensing the circadian signal, as well as a number of genes related to ROS response, e.g., thioredoxin (*trxA*), superoxide dismutase (*SOD2*), also showed increased expression under anoxia.

In phycospheric communities, the majority of genes were significantly downregulated under anoxia. However, some genes exhibited increased expression levels, such as the toxin-encoding gene *higB-1*, and *psbA* that encodes a photosystem II reaction center protein. In addition, multiple genes encoding histones (*H2A, H2B, H3* and *H4*) were upregulated [Fig. 4, **S4, Table S2**]. These proteins assist prokaryotic chromatin organization and may associate with overall decreased gene transcription in phycospheric bacteria (Pani and Nudler, 2023). On the contrary, transcripts of ABC transporter genes related to nitrate/nitrite/cyanate were not detected, likely suggesting decreased competitive advantages in terms of nutrient acquisition. Nonetheless, a range of genes involved in dissimilatory nitrate reduction, e.g., denitrification (*narGHI, napA*B, *nirK, norC* and *nosZ*) and DNRA (*napAB, nirBD* and *nrfA*), the assimilatory sulfate reduction pathway (*sat, cysDHIJN*), etc., were fully transcribed, though with lower expression levels under anoxia.

3.3. Characteristic gene expression of CA-associated microorganisms in the DO gradient

3.3.1. Overall transcriptional patterns of cyanobacteria and phycospheric bacteria

To investigate the transcriptional patterns of genes across the DO gradient, hierarchical clustering was performed, yielding five major clusters for cyanobacterial genes and five clusters of phycospheric bacteria-associated genes [Fig. 5, **Table S2**]. Some of these clusters shared similar patterns between cyanobacteria and phycospheric communities. For instance, both cyanobacterial cluster 3 (cyano-cluster 3) and bacterial cluster 2 (phyco-cluster 2) showed the highest transcriptional level under DO of 1.2 mg/L, and reduced expression with increasing DO. Similarly, the cyano-cluster 5 and phyco-cluster 3 showed the highest overall expression under DO 2.4 mg/L, and reduced expression with increasing DO. Therefore, the above clusters could represent characteristic transcriptional responses under hypoxic conditions. In addition, two clusters, namely cyano-cluster 2 and phyco-cluster 1, shared an opposite transcriptional trend, with increased expression toward higher DO, suggesting the associated genes were more actively transcribed under oxic conditions [Fig. 5]. Hence, these two clusters represented transcriptional responses to oxic conditions.

Functional analyses suggest these pairs of cyanobacterial and phycospheric clusters enriched distinct metabolic pathways [Fig. 5, **Table S2**]. Nonetheless, within the same cyanobacterial and phycospheric gene-cluster pair, enrichment of similar metabolic pathways was observed, suggesting conserved transcriptional regulatory patterns under different DO levels. For instance, both cyano-cluster 3 and phyco-cluster 2 enriched genes related to oxidative phosphorylation. Yet cyano-cluster 3 uniquely enriched fermentation-related genes (acetate kinase *ackA* and pyruvate-ferredoxin/flavodoxin oxidoreductase *por*) and pantothenate biosynthesis genes. Both cyano-cluster 5 and phyco-cluster 3 contained a range of genes related to biosynthesis of cofactors, ABC transporters, and biosynthesis of amino acids; while phyco-cluster 3 uniquely featured genes involved in DNA replication and N-glycan biosynthesis. Moreover, both cyano-cluster 2 and phyco-cluster 1 contained genes encoding two-component systems, amino acid synthases, and those related to carbon metabolism; while cyano-cluster 2 specifically enriched genes related to biosynthesis of a series secondary metabolites (e.g., tropane, piperidine, and pyridine alkaloid). Collectively, these results revealed both consistent and organism-specific responses to different oxygen conditions by the cyanobacterial and

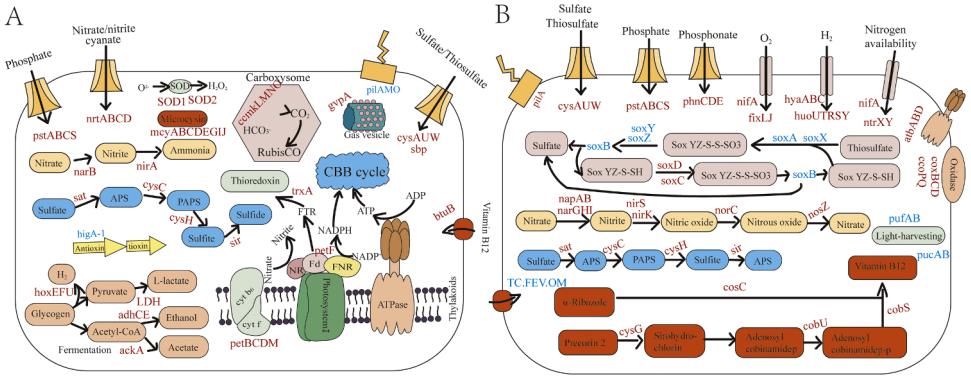

Fig. 4. Schematic metabolic diagrams of cyanobacteria (A) and phycospheric bacteria (B) in response to different redox conditions. Genes marked in red showed higher transcriptional activities under hypoxic or anoxic conditions, while genes marked in blue showed higher transcriptional activities under oxic conditions.

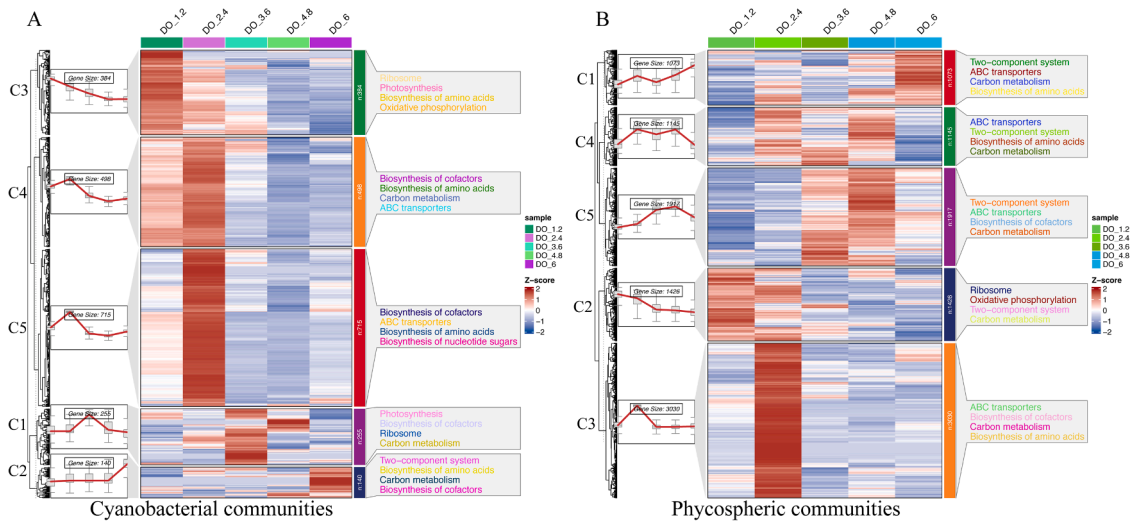

Fig. 5. Clustering analysis of functional gene expression patterns in cyanobacteria (A) and phycospheric communities (B) under different DO conditions. Vertical color bars on the right of each heatmap represent different gene clusters. C1 to C5 represent cyano-clusters 1 to 5 (A) and phyco-clusters 1 to 5 (B), respectively. Z-score represents standardized transcriptional abundance, calculated as (x - μ) / σ, where x is the observed value, μ is the mean, and σ is the standard deviation. The enriched metabolic pathways in each cluster were labeled on the right side of the heatmaps.

phycospheric communities.

3.3.2. *Characteristic transcriptional responses of CA-associated microorganisms under hypoxic conditions*

Both cyano-cluster 3 and phyco-cluster 2 exhibited favorable expression under hypoxic conditions, yet clade-specific gene expression patterns were also evident. In cyano-cluster 3, the highly expressed genes were mainly related to the photosynthetic electron transport chain and oxidative stress alleviation. These include genes encoding phycocyanin synthase (*cpcA*), photosystem II CP47 chlorophyll apoprotein

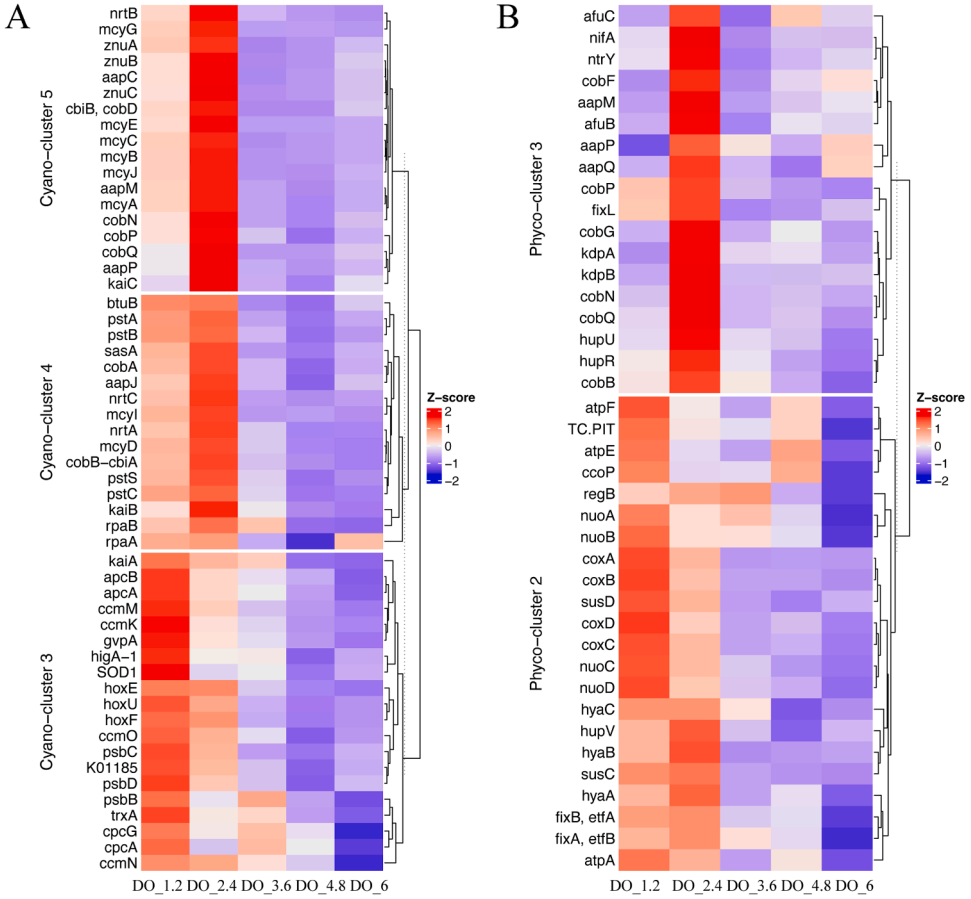

Fig. 6. Transcriptional patterns of representative genes under hypoxic conditions in cyanobacteria (A) and phycospheric bacteria (B). The color represents normalized transcriptional abundance for each gene.

(*psbBCD*, among others), allophycocyanin (*apcAB*), phycobilisome (*cpcG*), as well as thioredoxin (*trxA*) and superoxide dismutase (*SOD1*). Notably, within cyano-cluster 3, *gvpA*—which encodes the gas vesicle structural protein (GVP)—showed an approximately three-fold increase in expression as DO dropped from 6 mg/L to 1.2 mg/L [Fig. 6**A, Table S2**]. Other genes in this cluster were linked to carbon dioxide concentrating (*ccmKMNO*), hydrogenases (*hoxEFU*) and antitoxin (*higA-1*) mechanisms. Additionally, the lysozyme-encoding gene (K01185), often associated with antagonistic interactions, was also highly expressed. For phyco-cluster 2, the highly expressed genes were predominantly related to oxidative phosphorylation. This include the whole NADH-quinone oxidoreductase synthesis (*nuoABCD*, among others) operon, as well as those related to synthesis of ATPase (*atpAEF*, among others), cytochrome *c* oxidase (*coxABCD*, among others) and *cbb*3-type cytochrome *c* oxidase (*ccoP*), along with electron transfer flavoproteins such as *etfAB* [Fig. 6**B, Table S2**]. In addition, genes involved in response to environmental stimuli (such as nutrient acquisition and stress response mechanisms) were found in this cluster, including those for synthesizing the starch-binding outer membrane protein (*susCD*), inorganic phosphate transporter (*TC.PIT*), and redox signals response regulator (*regB*). These findings demonstrate that both cyanobacteria and phycospheric communities actively responded to changes of DO by adjusting their transcriptional activities.

Cyano-cluster 4, 5, along with phyco-cluster 3, also showed favorable expression under hypoxic conditions, with peak expression at DO 2.4 mg/L [Fig. 5, **Table S2**]. These clusters were enriched in genes related to nutrient acquisition and antagonistic defense, suggesting potential resource competition between cyanobacteria and phycospheric microbes. Specifically, cyano-clusters 4 and 5 included a series of genes involved in the uptake of nitrate/nitrite/cyanate (*nrtABC*), phosphate (*pstABCS*), zinc (*znuABC*) and general L-amino acids (*aapCJMP*) [Fig. 6**A, Table S2**], as well as multiple microcystin synthesis-related genes (*mcyABCDEGIJ*). Circadian regulation genes, such as the response regulator (*rpaAB*), circadian clock protein (*kaiBC*), and clock-associated histidine kinase (*sasA*) genes, were also found in this cluster, with *rpaB* and *kaiB* of particularly high expression levels (top 70) [**Table S2**]. In phyco-cluster 3, genes associated with acquisition of general L-amino acids (*aapMPQ*) and iron (*afuBC*) were similarly expressed, along with genes involved in two-component regulatory systems responsive to environmental signals such as hydrogen (*hupUR*), oxygen (*fixL* and *nifA*), nitrogen (*ntrY*), and potassium (*kdpAB*) [Fig. 6**B, Table S2**]. This cluster also contained a suite of cobalamin (vitamin B_{12}) biosynthesis genes including *cobBGFNPQ*, whereas the corresponding cyano-clusters 4 and 5 expressed a number of cobalamin synthesis-related genes (such as *cobNPQ*) but lacked key components such as *cobG* and *cobF*. Collectively, these finding suggest intense competition for nitrogen and iron under hypoxia, but also a potential beneficial role of phycospheric bacteria in supporting cyanobacterial growth through vitamin B_{12} provision.

3.3.3. Transcriptional response of CA-associated microorganisms to oxic conditions

Two clusters, namely cyano-cluster 2 and phyco-cluster 1, shared a similar transcriptional trend with elevated expression with increasing DO, representing characteristic transcriptional response to oxic conditions [Fig. 5**, Table S2**]. For cyano-cluster 2, the *pilA* gene showed the highest transcriptional abundance. Interestingly, the gene *higB-1* encoding a toxin showed increased expression with rising DO, while the gene encoding the antitoxin (*higA-1*) clustered in cyano-cluster 3 and showed preferential expression under hypoxia [Fig. 4**A, Table S2**]. These opposing trends suggest that HigA may more effectively counteract the toxic effects of HigB under oxygen-deficient rather than oxic conditions (Wood and Wood, 2016), potentially contributing to the overall increased transcriptional activities of cyanobacteria at low DO levels. In phyco-cluster 1, the genes with the highest transcriptional abundances were those encoding iron complex outer membrane receptor proteins (*TC.FEV.OM*). Additionally, genes related to synthesis of photosynthetic pigments, such as those encoding the light-harvesting complex (*pufAB*) and light-harvesting protein (*pucAB*), also exhibited high transcriptional abundances in this cluster. Moreover, as DO increased, increased expression was observed for genes encoding L-cysteine S-thiosulfotransferase (*soxAX*), sulfur-oxidizing protein (*soxYZ*), and S-sulfosulfanyl-L-cysteine sulfohydrolase (*soxB*) [Fig. 4**B, Table S2**]. This suggests enhanced potential of thiosulfate oxidation to sulfate by phycospheric bacteria with the rise in DO.

3.4. Physiological response of microcystis under anoxic, hypoxic and oxic conditions

The physiological responses of *Microcystis* under anoxic, hypoxic (DO $\approx$ 1.5 mg/L) and oxic (DO $\approx$ 7.4 mg/L) conditions were next assessed after 24 h of incubation with the strain FACHB-915. As a result, *Microcystis* cell density increased relative to the pre-incubation baseline in oxic and hypoxic conditions, whereas no growth was observed under anoxia [Fig. 7]. Conversely, increased ROS level, EPS content and alcohol production was observed under anoxia and hypoxic conditions, in line with elevated ROS response- and fermentation-related gene expression in *Microcystis* at lower DO levels.

4. Discussion

4.1. Shift of active CA-associated communities in response to DO change

Based on sequencing of the 16S rRNA amplicons and the metatranscriptomes, both cyanobacterial genera *Microcystis* and *Pseudanabaena* exhibited high metabolic activities under anoxia and hypoxia, underscoring their adaptive strategies to cope with oxygen-deficient conditions. Notably, *Microcystis* upregulated a range of genes related to ROS resistance under hypoxia and anoxia, such as *SOD1* (superoxide dismutase), *petF* (ferredoxin), *trxA* (thioredoxin) (Anjou et al., 2024), as well as genes encoding the thylakoid membrane-localized cytochrome *c* oxidase (*coxBCD*), which exhibits peroxidase activity (Howitt and Vermaas, 1998; Ludwig et al., 2001). The genes related to microcystin biosynthesis also showed elevated expression with decreased DO, with microcystin molecules shown to help alleviate ROS and aid cyanobacterial survival in sediments(Wei et al., 2024). These observations together suggest that oxygen deficiency can trigger ROS stress in cyanobacteria, challenging the common recognition that ROS are typically produced under oxic conditions. While ROS are often viewed as abiotic photochemical byproducts of sunlight exposure in surface waters or as biological products via the photosynthetic electron transport chain (Andrews et al., 2000), they can also be produced by non-photosynthetic microorganisms in darkness (Diaz et al., 2013). However, reports on ROS production under hypoxic conditions remain scarce. Previous research has found increased ROS response in *Microcystis* under anoxic conditions based on metatranscriptomic analysis (Chen et al., 2023). In addition, hypoxia-induced ROS production has been documented in mammalian cells, potentially linked to altered activity of the respiratory electron transport chain (Chen et al., 2018). In this study, both elevated ROS levels in *Microcystis* cultures by direct measurement and upregulation of ROS response-related genes in colonial *Microcystis* was detected under low-oxygen conditions, reinforcing the notion that managing oxidative stress is a critical physiological challenge for cyanobacteria in oxygen-depleted environments.

Response to different DO levels was also reflected in shifts of the transcriptional activities of the phycospheric bacterial communities. For instance, both *Rheinheimera* and *Flavobacterium* showed increased transcriptional activities as DO rose, as observed in both the 16S rRNA and metatranscriptomic profiles. In contrast to *Microcystis, Rheinheimera* exhibited markedly reduced expression of the ROS-response genes under low-oxygen conditions, including *trxA* (thioredoxin), *tpx* (NADH-dependent peroxiredoxin), *SOD2* (superoxide dismutase), *gpx*

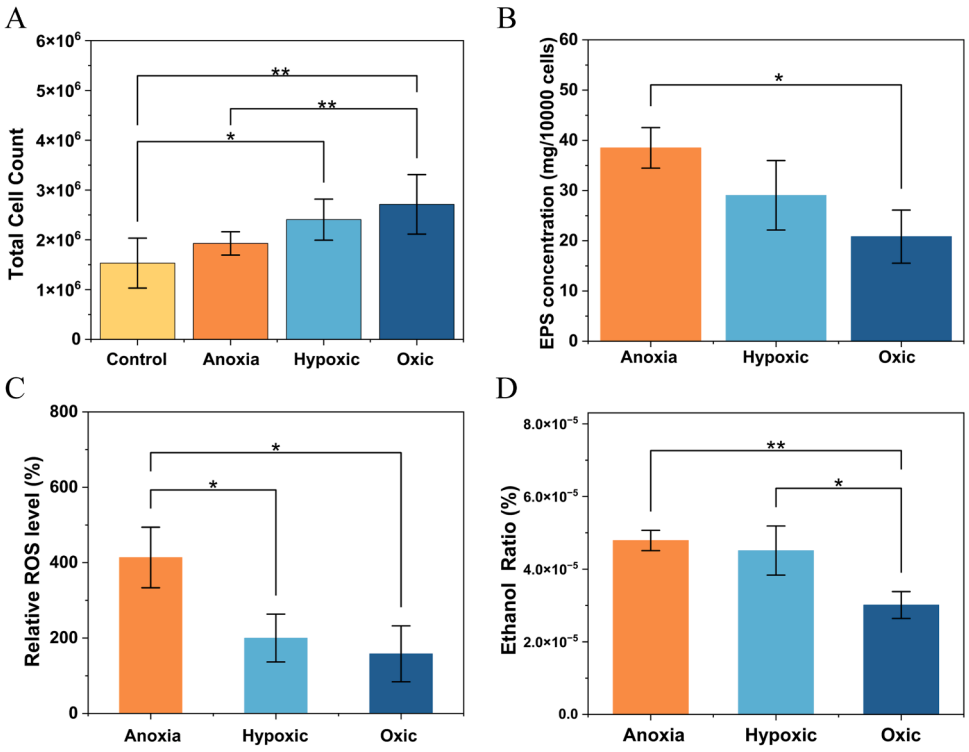

Fig. 7. Characterization of cell count (A), EPS content (B), ROS level (C), and alcohol production (D) of *Microcystis* under anoxic, hypoxic, and oxic conditions for 24 h. * and ** denote statistically significant differences by T-test, with $p \leq 0.05$ and $p \leq 0.01$, respectively.

(glutathione peroxidase), etc., suggesting a diminished capacity to withstand oxidative stress [**Table S3**]. In the meanwhile, *Flavobacterium* displayed significant upregulation of genes involved in central carbon metabolism, particularly under oxic conditions, consistent with its known ecological role as an active organic carbon degrader in aquatic systems (Lopez-Sánchez et al., 2024). These observations indicate that oxygen availability not only shaped the metabolic strategies of cyanobacteria but also governed the functional responses of the phycospheric communities.

4.2. *Cyanobacteria may employ O_2-independent alternative electron sink to cope with hypoxia and anoxia*

Cyanobacteria in CAs likely utilized nitrate, nitrite or sulfate as alternate electron acceptors under hypoxia or anoxia to alleviate the pressure of oxygen deficiency. Our results showed that cyanobacterial genes associated with assimilatory nitrate reduction and assimilatory sulfate reduction were highly transcribed under the anoxic condition, and the genes related to nitrate/nitrite/cyanate transport also exhibited increased expression as DO decreased. This implied that alternative electron transport receptors (nitrate and sulfate) may be used in compensation for oxygen deficiency (Froelich et al., 1979; Thamdrup et al., 2012). In our study, on one hand, elevated expression levels under low-oxygen conditions were observed in a number of genes encoding reductases that utilize ferredoxin as the electron transfer mediator [**Table S2**]. Such enzymes include ferredoxin-nitrite reductase (*nirA*), ferredoxin-thioredoxin reductase (FTRC), ferredoxin-$NADP^+$ reductase (*petH*), and sulfite reductase (*sir*), supporting the role of ferredoxin in mediating the transfer of excessive electrons to various reductases under oxygen deficiency (Iyanagi, 2022; Mondal and Bruce, 2018). On the other hand, the circadian clock-regulated transcription factor gene *rpaA* was also of higher transcription under hypoxia and anoxia. RpaA is known to regulate energy transfer from phycobilisomes to Photosystem I through direct interaction with ferredoxin (Hanke et al., 2011). The ferredoxin:RpaA interaction can be substantially affected by cellular redox state, with much stronger binding under reduced conditions (Hanke et al., 2011). This suggests that RpaA and ferredoxin may directly control energy transfer, and are influenced by both light/dark cycles and cellular redox state. Hence, activation of cyanobacterial *rpaA* gene expression under dark and anoxia likely facilitated ferredoxin-mediated electron transport, thereby promoting O_2-independent alternative electron transport under oxygen deficiency. It was worth mentioning that previous studies on ferredoxin-mediated electron sink were mostly related to the photosynthetic electron transport chain (Flores et al., 2005; Navarro et al., 2000). However, our research is the first to report high expression of ferredoxin and related reductase synthesis genes under anoxic conditions, providing novel insights into the metabolic mechanisms by which cyanobacteria resist oxygen-deficiency stress.

Furthermore, cyanobacteria in CAs enhance their fitness under oxygen deficient conditions by activating the fermentation processes, as evidenced by upregulation of genes encoding lactate dehydrogenase, alcohol dehydrogenase, and hydrogenase, along with increased alcohol production under low-oxygen treatments [Fig. 7**A**]. Fermentative metabolism in cyanobacteria under anoxia has been previously reported in several species, including *M. aeruginosa* (Moezelaar and Stal, 1994), *Microcoleus chthonoplastes* (Moezelaar et al., 1996), and *Nostoc* sp. (Margheri and Allotta, 1993). In our study, alcohol production by *Microcystis* was nonetheless detected under oxic conditions, consistent with previous documentation that enzymes involved in fermentative metabolism are already synthesized during growth under aerobic condition (Moezelaar and Stal, 1994). Collectively, these findings indicate that *Microcystis* is highly adapted to fluctuating redox environments, and can swiftly transition to fermentation-based metabolism when oxygen becomes limiting.

4.3. *Interactions between cyanobacteria and phycospheric microorganisms within CAs*

Oxygen-deficient conditions may alter the interaction dynamics

between cyanobacteria and their associated phycospheric bacteria. Previous studies have suggested nutrient competition can be a major driver of antagonistic interactions between these microbial groups (Seymour et al., 2017; Zheng et al., 2020). In this study, hypoxia was associated with increased transcription of genes involved in nitrogen and iron acquisition in both cyanobacterial and phycospheric communities, indicating intensified competition for these essential nutrients. Additionally, lysozyme-encoding genes were highly expressed in cyanobacteria under hypoxia and anoxia, suggesting potential activation of antimicrobial strategies. These findings together support intensified antagonistic interactions between cyanobacteria and phycospheric bacteria, likely associated with nutrient competition as DO decreased. Nonetheless, beneficial effect of phycospheric bacteria on cyanobacteria was evident. Genomic analyses have shown that approximately half of all microalgae are auxotrophs for cobalamin, yet requiring it as a cofactor for cobalamin-dependent methionine synthase (Croft et al., 2005). For those unable to synthesize it *de novo*, cobalamin must be acquired from the environment (Kazamia et al., 2012). In this study, while both cyanobacteria and phycospheric bacteria expressed cobalamin biosynthesis genes under hypoxic conditions, key genes were absent in cyanobacteria but actively transcribed in phycospheric bacteria [Fig. 6, **Table S2**]. Concurrent expression of the cobalamin transporter gene (*btuB*) in cyanobacteria further supports a cross-feeding interaction, suggesting that phycospheric bacteria enhance cyanobacterial growth by supplying essential vitamins like cobalamin.

4.4. Gene expression of CAs facilitates evasion from oxygen-deficient environment

CA-associated communities may adopt other strategies through promoting motility to 'escape' oxygen-deficient environment. In this study, *gvpA*, which encodes the major structural protein of gas vesicle, was highly expressed in *Microcystis* under decreased DO levels. Gas vesicles are gas-filled protein particles that enable buoyancy regulation in cyanobacteria and other microorganisms (Strunk et al., 2011). GvpA forms the bulk of the vesicle wall—typically over 90 %—while GvpC plays a minor stabilizing role (Ezzeldin et al., 2012). Although *gvpC* transcripts were not detected in our metatranscriptomic data, *gvpA* transcripts were consistently abundant across all conditions, ranking among the top two under anoxia and within the top 20 under hypoxic and oxic conditions [Table S2]. The increased *gvpA* expression under low DO suggests cyanobacteria may utilize gas vesicle formation to escape from oxygen-deficient environment. While previous studies have shown that *gvp* gene expression can be influenced by light, CO_2 concentration, cell density, temperature, pH, and salinity (Pfeifer, 2012), our findings provide the first evidence that DO levels may also regulate GVP-associated gene expression in cyanobacteria, potentially aiding colony migration away from hypoxic zones.

5. Conclusions

The ecological success of CAs during cyanobacterial blooms depends on their ability to adapt to changing DO levels. In this study, combined transcriptional and metabolic analyses across an oxic–hypoxic–anoxic gradient revealed unexpectedly high ROS stress under oxygen-deficient conditions, and several active cyanobacterial responses, including upregulation of ROS scavenging enzymes, fermentative metabolism, deployment of alternative electron sink, and increased gas vesicle synthesis to escape hypoxia. Intensified nutrient competition with phycospheric bacteria was also observed, even as these partners continued to supply cobalamin. Together, these insights illuminate the multifaceted strategies CAs employ to sense, respond to, and thrive under fluctuating DO conditions.

CRediT authorship contribution statement

Dezhuang Gao: Writing – original draft, Methodology, Investigation, Formal analysis, Data curation. **Zhijie Chen:** Writing – original draft, Methodology, Investigation, Formal analysis, Data curation. **Yuan Ma:** Methodology, Investigation. **Ruiyu Wang:** Investigation. **Jie Deng:** Writing – review & editing, Funding acquisition, Conceptualization.

Declaration of competing interest

The authors declare no conflict of interest.

Acknowledgements

This work was supported by Natural Science Foundation of China [grant numbers 91951104, 42177098, and 31800424, and the Fundamental Research Funds for the Central Universities.

Supplementary materials

Supplementary material associated with this article can be found, in the online version, at doi:10.1016/j.hal.2025.102922.

Data availability

Data will be made available on request.

References

Andrews, S.S., Caron, S., Zafiriou, O.C., 2000. Photochemical oxygen consumption in marine waters: a major sink for colored dissolved organic matter? Limnol. Oceanogr. 45 (2), 267–277.

Anjou, C., Lotoux, A., Morvan, C., Martin-Verstraete, I., 2024. From ubiquity to specificity: the diverse functions of bacterial thioredoxin systems. Environ. Microbiol. 26 (6), e16668.

Bianchi, D., Weber, T.S., Kiko, R., Deutsch, C., 2018. Global niche of marine anaerobic metabolisms expanded by particle microenvironments. Nat. Geosci. 11 (4), 263–268.

Biller, S.J., Coe, A., Chisholm, S.W., 2016. Torn apart and reunited: impact of a heterotroph on the transcriptome of *Prochlorococcus*. ISME J. 10 (12), 2831–2843.

Bokulich, N.A., Kaehler, B.D., Rideout, J.R., Dillon, M., Bolyen, E., Knight, R., Huttley, G. A., Caporaso, J.G., 2018. Optimizing taxonomic classification of marker-gene amplicon sequences with QIIME 2's q2-feature-classifier plugin. Microbiome 6.

Bolger, A.M., Lohse, M., Usadel, B., 2014. Trimmomatic: a flexible trimmer for Illumina sequence data. Bioinformatics 30 (15), 2114–2120.

Bolyen, E., Rideout, J.R., Dillon, M.R., Bokulich, N., Abnet, C.C., Al-Ghalith, G.A., Alexander, H., Alm, E.J., Arumugam, M., Asnicar, F., Bai, Y., Bisanz, J.E., Bittinger, K., Brejnrod, A., Brislawn, C.J., Brown, C.T., Callahan, B.J., Caraballo-Rodriguez, A.M., Chase, J., Cope, E.K., Da Silva, R., Diener, C., Dorrestein, P.C., Douglas, G.M., Durall, D.M., Duvallet, C., Edwardson, C.F., Ernst, M., Estaki, M., Fouquier, J., Gauglitz, J.M., Gibbons, S.M., Gibson, D.L., Gonzalez, A., Gorlick, K., Guo, J.R., Hillmann, B., Holmes, S., Holste, H., Huttenhower, C., Huttley, G.A., Janssen, S., Jarmusch, A.K., Jiang, L.J., Kaehler, B.D., Bin Kang, K., Keefe, C.R., Keim, P., Kelley, S.T., Knights, D., Koester, I., Kosciolek, T., Kreps, J., Langille, M.G. I., Lee, J., Ley, R., Liu, Y.X., Loftfield, E., Lozupone, C., Maher, M., Marotz, C., Martin, B.D., McDonald, D., McIver, L.J., Melnik, A.V., Metcalf, J.L., Morgan, S.C., Morton, J.T., Naimey, A.T., Navas-Molina, J.A., Nothias, L.F., Orchanian, S.B., Pearson, T., Peoples, S.L., Petras, D., Preuss, M.L., Pruesse, E., Rasmussen, L.B., Rivers, A., Robeson, M.S., Rosenthal, P., Segata, N., Shaffer, M., Shiffer, A., Sinha, R., Song, S.J., Spear, J.R., Swafford, A.D., Thompson, L.R., Torres, P.J., Trinh, P., Tripathi, A., Turnbaugh, P.J., Ul-Hasan, S., vander Hooft, J.J.J., Vargas, F., Vazquez-Baeza, Y., Vogtmann, E., von Hippel, M., Walters, W., Wan, Y.H., Wang, M.X., Warren, J., Weber, K.C., Williamson, C.H.D., Willis, A.D., Xu, Z.Z., Zaneveld, J.R., Zhang, Y.L., Zhu, Q.Y., Knight, R., Caporaso, J.G., 2019. Reproducible, interactive, scalable and extensible microbiome data science using QIIME 2. Nat. Biotechnol. 37 (8), 852–857.

Buchfink, B., Reuter, K., Drost, H.G., 2021. Sensitive protein alignments at tree-of-life scale using DIAMOND. Nat. Methods 18 (4), 366–368.

Callahan, B.J., McMurdie, P.J., Rosen, M.J., Han, A.W., Johnson, A.J.A., Holmes, S.P., 2016. DADA2: high-resolution sample inference from Illumina amplicon data. Nat. Method 13 (7), 581–583.

Callieri, C., Slabakova, V., Dzhembekova, N., Slabakova, N., Peneva, E., Cabello-Yeves, P. J., Di Cesare, A., Eckert, E.M., Bertoni, R., Corno, G., Salcher, M.M., Kamburska, L., Bertoni, F., Moncheva, S., 2019. The mesopelagic anoxic Black Sea as an unexpected habitat for challenges our understanding of global "deep red fluorescence. ISME J. 13 (7), 1676–1687.

Caporaso, J.G., Lauber, C.L., Walters, W.A., Berg-Lyons, D., Huntley, J., Fierer, N., Owens, S.M., Betley, J., Fraser, L., Bauer, M., Gormley, N., Gilbert, J.A., Smith, G.,

Knight, R., 2012. Ultra-high-throughput microbial community analysis on the Illumina HiSeq and MiSeq platforms. ISME J. 6 (8), 1621–1624.
Chen, R., Lai, U.H., Zhu, L., Singh, A., Ahmed, M., Forsyth, N.R., 2018. Reactive oxygen species formation in the brain at different oxygen levels: the role of hypoxia inducible factors. Front. Cell. Dev. Biol. 6, 2018.
Chen, Z.J., Huang, Y.Y., Shen, Y.S., Zhang, J.Y., Deng, J., Chen, X.C., 2023. Denitrification shifted autotroph-heterotroph interactions in *Microcystis* aggregates. Environ. Res. 231.
Christie-Oleza, J.A., Sousoni, D., Lloyd, M., Armengaud, J., Scanlan, D.J., 2017. Nutrient recycling facilitates long-term stability of marine microbial phototroph–heterotroph interactions. Nat. Microbiol. 2 (9), 17100.
Chuang, D.S.W., Liao, J.C., 2021. Role of cyanobacterial phosphoketolase in energy regulation and glucose secretion under dark anaerobic and osmotic stress conditions. Metab. Eng. 65, 255–262.
Croft, M.T., Lawrence, A.D., Raux-Deery, E., Warren, M.J., Smith, A.G., 2005. Algae acquire vitamin B_{12} through a symbiotic relationship with bacteria. Nature 438 (7064), 90–93.
Deben, C., Zwaenepoel, K., Boeckx, C., Wouters, A., Pauwels, P., Peeters, M., Lardon, F., Baay, M., Deschoolmeester, V., 2013. Expression analysis on archival material revisited: isolation and quantification of RNA extracted from FFPE samples. Diagn. Mol. Pathol. 22 (1), 59–64.
Diaz, J.M., Hansel, C.M., Voelker, B.M., Mendes, C.M., Andeer, P.F., Zhang, T., 2013. Widespread production of extracellular superoxide by heterotrophic bacteria. Science 340 (6137), 1223–1226.
Ezzeldin, H.M., Klauda, J.B., Solares, S.D., 2012. Modeling of the major gas vesicle protein, GvpA: from protein sequence to vesicle wall structure. J. Struct. Biol. 179 (1), 18–28.
Feng, L., Wang, Y., Hou, X., Qin, B., Kutser, T., Qu, F., Chen, N., Paerl, H.W., Zheng, C., 2024. Harmful algal blooms in inland waters. Nat. Rev. Earth Environ. 5 (9), 631–644.
Flores, E., Frías, J.E., Rubio, L.M., Herrero, A., 2005. Photosynthetic nitrate assimilation in cyanobacteria. Photosynth. Res. 83 (2), 117–133.
Froelich, P.N., Klinkhammer, G.P., Bender, M.L., Luedtke, N.A., Heath, G.R., Cullen, D., Dauphin, P., Hammond, D., Hartman, B., Maynard, V., 1979. Early oxidation of organic matter in pelagic sediments of the eastern equatorial Atlantic: suboxic diagenesis. Geochim. Cosmochim. Ac. 43 (7), 1075–1090.
Fu, L.M., Niu, B.F., Zhu, Z.W., Wu, S.T., Li, W.Z., 2012. CD-HIT: accelerated for clustering the next-generation sequencing data. Bioinformatics 28 (23), 3150–3152.
Gobler, C.J., 2020. Climate change and harmful algal blooms: insights and perspective. Harmful Algae 91, 101731.
Guerrero, R., Berlanga, M., 2016. From the cell to the ecosystem: the physiological evolution of symbiosis. Evol. Biol. 43 (4), 543–552.
Gutthann, F., Egert, M., Marques, A., Appel, J., 2007. Inhibition of respiration and nitrate assimilation enhances photohydrogen evolution under low oxygen concentrations in *synechocystis* sp. PCC6803. Bba-Bioenergetics. 1767 (2), 161–169.
Hajdu, S., Höglander, H., Larsson, U., 2007. Phytoplankton vertical distributions and composition in Baltic Sea cyanobacterial blooms. Harmful. Algae 6 (2), 189–205.
Hanke, G.T., Satomi, Y., Shinmura, K., Takao, T., Hase, T., 2011. A screen for potential ferredoxin electron transfer partners uncovers new, redox dependent interactions. Bba-Proteins Proteom 1814 (2), 366–374.
He, C.-S., Ding, R.-R., Chen, J.-Q., Li, W.-Q., Li, Q., Mu, Y., 2020. Interactions between nanoscale zero valent iron and extracellular polymeric substances of anaerobic sludge. Water Res. 178, 115817.
Hoffmann, D., Maldonado, J., Wojciechowski, M.F., Garcia-Pichel, F., 2015. Hydrogen export from intertidal cyanobacterial mats: sources, fluxes and the influence of community composition. Environ. Microbiol. 17 (10), 3738–3753.
Howitt, C.A., Vermaas, W.F.J., 1998. Quinol and cytochrome oxidases in the cyanobacterium *synechocystis* sp. PCC6803. Biochem.-Us 37 (51), 17944–17951.
Hyatt, D., Chen, G.L., LoCascio, P.F., Land, M.L., Larimer, F.W., Hauser, L.J., 2010. Prodigal: prokaryotic gene recognition and translation initiation site identification. BMC Bioinform. 11, 119.
Iyanagi, T., 2022. Roles of ferredoxin-NADP(+) oxidoreductase and flavodoxin in NAD(P)H-dependent electron transfer systems. Antioxidants (Basel) 11 (11), 2143.
Ji, M.Z., Zhou, J.Y., Li, Y., Ma, K., Song, W., Li, Y.Y., Zhou, J.Z., Tu, Q.C., 2024. Biodiversity of mudflat intertidal viromes along the Chinese coasts. Nat. Commun. 15 (1), 8611.
Kanehisa, M., Goto, S., Kawashima, S., Okuno, Y., Hattori, M., 2004. The KEGG resource for deciphering the genome. Nucl. Acids Res. 32, D277–D280.
Kazamia, E., Czesnick, H., Thi, T.V.N., Croft, M.T., Sherwood, E., Sasso, S., Hodson, S.J., Warren, M.J., Smith, A.G., 2012. Mutualistic interactions between vitamin B_{12}-dependent algae and heterotrophic bacteria exhibit regulation. Environ. Microbiol. 14 (6), 1466–1476.
Klawonn, I., Bonaglia, S., Brüchert, V., Ploug, H., 2015. Aerobic and anaerobic nitrogen transformation processes in N_2-fixing cyanobacterial aggregates. ISME J 9 (6), 1456–1466.
Kopylova, E., Noé, L., Touzet, H., 2012. SortMeRNA: fast and accurate filtering of ribosomal RNAs in metatranscriptomic data. Bioinformatics 28 (24), 3211–3217.
Langmead, B., Salzberg, S.L., 2012. Fast gapped-read alignment with Bowtie 2. Nat. Methods 9 (4), 357–359.
Latifi, A., Ruiz, M., Zhang, C.-C., 2009. Oxidative stress in cyanobacteria. Fems Microbiol. Rev. 33 (2), 258–278.
Latour, D., Sabido, O., Salencon, M.J., Giraudet, H., 2004. Dynamics and metabolic activity of the benthic cyanobacterium *microcystis aeruginosa* in the Grangent reservoir (France). J. Plankton Res. 26 (7), 719–726.
Le, S., Josse, J., Husson, F., 2008. FactoMineR: an R package for multivariate analysis. J. Stat. Softw. 25 (1), 1–18.
Lopez-Sánchez, R., Rebollar, E.A., Gutierrez-Rios, R.M., Garciarrubio, A., Juarez, K., Segovia, L., 2024. Metagenomic analysis of carbohydrate-active enzymes and their contribution to marine sediment biodiversity. World J. Microb. Biot. 40 (3), 95.
Ludwig, B., Bender, E., Arnold, S., Hüttemann, M., Lee, I., Kadenbach, B., 2001. Cytochrome c oxidase and the regulation of oxidative phosphorylation. Chembiochem 2 (6), 392–403.
Ma, J.R., Brookes, J.D., Qin, B.Q., Paerl, H.W., Gao, G., Wu, P., Zhang, W., Deng, J.M., Zhu, G.W., Zhang, Y.L., Xu, H., Niu, H.L., 2014. Environmental factors controlling colony formation in blooms of the cyanobacteria *microcystis* spp. in Lake Taihu, China. Harmful Algae 31, 136–142.
Margheri, M.C., Allotta, G., 1993. Homoacetic fermentation in the cyanobacterium *nostoc* sp. strain cc from *Cycas circinalis*. Fems Microbiol. Lett. 111 (2), 213–217.
McDonald, D., Price, M.N., Goodrich, J., Nawrocki, E.P., DeSantis, T.Z., Probst, A., Andersen, G.L., Knight, R., Hugenholtz, P., 2012. An improved greengenes taxonomy with explicit ranks for ecological and evolutionary analyses of bacteria and archaea. ISME J. 6 (3), 610–618.
Moezelaar, R., Bijvank, S.M., Stal, L.J., 1996. Fermentation and sulfur reduction in the mat-building byanobacterium *microcoleus chthonoplastes*. Appl. Environ. 62 (5), 1752–1758.
Moezelaar, R., Stal, L.J., 1994. Fermentation in the unicellular cyanobacterium *microcystis* PCC7806. Arch. Microbiol. 162 (1), 63–69.
Mondal, J., Bruce, B.D., 2018. Ferredoxin: the central hub connecting photosystem I to cellular metabolism. Photosynthetica 56 (1), 279–293.
Morris, J.J., Johnson, Z.I., Szul, M.J., Keller, M., Zinser, E.R., 2011. Dependence of the cyanobacterium on hydrogen peroxide scavenging microbes for growth at the ocean's surface. Plos One 6 (2), e16805.
Navarro, F., Martín-Figueroa, E., Candau, P., Florencio, F.J., 2000. Ferredoxin-dependent iron-sulfur flavoprotein glutamate synthase (GlsF) from the cyanobacterium *synechocystis* sp PCC6803: expression and assembly in *Escherichia coli*. Arch. Biochem. Biophys. 379 (2), 267–276.
Paerl, H.W., Hall, N.S., Calandrino, E.S., 2011. Controlling harmful cyanobacterial blooms in a world experiencing anthropogenic and climatic-induced change. Sci. Total Environ. 409 (10), 1739–1745.
Pani, B., Nudler, E., 2023. Bacterial histones unveiled. Nat. Microbiol. 8 (11), 1939–1941.
Pfeifer, F., 2012. Distribution, formation and regulation of gas vesicles. Nat. Rev. Microbiol. 10 (10), 705–715.
Quinlan, A.R., Hall, I.M., 2010. BEDTools: a flexible suite of utilities for comparing genomic features. Bioinformatics 26 (6), 841–842.
Rai, P., Pathania, R., Bhagat, N., Bongirwar, R., Shukla, P., Srivastava, S., 2025. Current insights into molecular mechanisms of environmental stress tolerance in cyanobacteria. World J. Microbio. Biotechnol. 41 (2), 53.
Robarts, R.D., Zohary, T., 1987. Temperature effects on photosynthetic capacity, respiration, and growth rates of bloom-forming cyanobacteria. N. Z. J. Mar. Freshwater Res. 21 (3), 391–399.
Seymour, J.R., Amin, S.A., Raina, J.B., Stocker, R., 2017. Zooming in on the phycosphere: the ecological interface for phytoplankton-bacteria relationships. Nat. Microbiol. 2 (7), 17065.
Strunk, T., Hamacher, K., Hoffgaard, F., Engelhardt, H., Zillig, M.D., Faist, K., Wenzel, W., Pfeifer, F., 2011. Structural model of the gas vesicle protein GvpA and analysis of GvpA mutants. Mol. Microbiol. 81 (1), 56–68.
Thamdrup, B., Dalsgaard, T., Revsbech, N.P., 2012. Widespread functional anoxia in the oxygen minimum zone of the Eastern South Pacific. Deep-Sea Res. Pt. I 65, 36–45.
Walsby, A.E., Booker, M.J., 1980. Changes in buoyancy of a planktonic blue-green alga in response to light intensity. British Phycolog. J. 15 (4), 311–319.
Walsby, A.E., Hayes, P.K., Boje, R., Stal, L.J., 1997. The selective advantage of buoyancy provided by gas vesicles for planktonic cyanobacteria in the Baltic Sea. New Phytol. 136 (3), 407–417.
Wei, N., Hu, C., Dittmann, E., Song, L., Gan, N., 2024. The biological functions of microcystins. Water Res. 262, 122119.
Wood, T.L., Wood, T.K., 2016. The HigB/HigA toxin/antitoxin system of *Pseudomonas aeruginosa* influences the virulence factors pyochelin, pyocyanin, and biofilm formation. Microbiologyopen 5 (3), 499–511.
Wu, T.H., Dai, R., Chu, Z.S., Cao, J., 2023. Rapid recovery of buoyancy in eutrophic environments indicates that cyanobacterial blooms cannot be effectively controlled by simply collapsing gas vesicles alone. Water-Sui. 15 (10), 1898.
Xiao, M., Li, M., Reynolds, C.S., 2018. Colony formation in the cyanobacterium *microcystis*. Biol. Rev. 93 (3), 1399–1420.
Yang, Y., Chen, H., Lu, J.F., 2023. Inactivation of algae by visible-light-driven modified photocatalysts: a review. Sci. Total Environ. 858, 159640.
Zhang, J., 2022. ClusterGVis: One-step to Cluster and Visualize Gene Expression Matrix. CRAN (R package).
Zheng, Q., Wang, Y., Lu, J.Y., Lin, W.X., Chen, F., Jiao, N.Z., 2020. Metagenomic and metaproteomic insights into photoautotrophic and heterotrophic interactions in a culture. Mbio. 11 (1).